IRON SUBSTITUTION IN SOIL AND SYNTHETIC ANATASE

U. Schwertmann, J. Friedl, G. Pfab, and A. U. Gehring

Lehrstuhl für Bodenkunde, Technische Universität München,
D-80350 Freising-Weihenstephan

Abstract—Iron^{III} for Ti^{IV} substitution in the structure of pedogenic and synthetic anatase of up to Fe/(Ti+Fe) 0.1 mol/mol was indicated by an increase in unit cell size as measured by XRD line shifts. Mössbauer- and electron paramagnetic resonance spectra at both, 298 K and 4.2 K supported this by the presence of signals typical for octahedrally coordinated Fe^{III} in a diamagnetic matrix. Charge compensation was achieved by structural OH, as indicated by FTIR bands at 3360 and 960 cm^{-1}, which were absent in pure anatase and which disappeared on heating. The weight loss on heating amounted to ca. 0.5 mol H$_2$O/mol Fe. At 600°C structural Fe was ejected, the unit cell size decreased to that of pure anatase, and pseudobrookite, Fe$_2$TiO$_5$, was formed.

Key Words—Anatase, Crystal chemistry, EPR, Fe substitution, FTIR, Mössbauer, OH–O-substitution, Pseudobrookite, TA, TEM, XRD.

INTRODUCTION

Mean Ti concentrations in various soils range between 1.5 and 29.3 g/kg (Milnes and Fitzpatrick 1989). Titanium is found in fairly stable residual minerals such as ilmenite, titano-magnetite and rutile, but also in pedogenic minerals of which anatase has been most frequently identified. Pseudorutile and titano-maghemite are two others. Anatase is considered a weathering product of Ti-bearing, Fe-rich silicates (biotites, pyroboles) and sphene (Milnes and Fitzpatrick 1989). It can be assumed, therefore, that anatase in the weathering environment forms in the presence of an ample supply of Fe. If not sufficient to create Fe-Ti-phases, like pseudorutile, the question arises if Fe^{III} may enter the tetragonal structure of anatase in measurable amounts. To the best of our knowledge, the literature holds no proof of Fe-for-Ti substitution in natural anatase except that Fe has been noted as a trace constituent (Deer *et al* 1962).

Fitzpatrick *et al* (1978) synthesized Ti-Fe-mixed phases from coprecipitates at 70°C and obtained anatase as the sole phase between Ti/(Ti+Fe) ratios of 0.7 and 1.0. The Fe was no longer oxalate extractable, and the XRD peaks became broader as Fe content increased. On these grounds, structural incorporation of Fe was suggested. A slight shift of the 101 X-ray peak toward higher d-values was indeed visible, but was not noticed by the authors. A similar line shift was recently observed with anatases from deep saprolites of lateritic profiles on basalt of the Jos Plateau, central Nigeria (Zeese *et al* 1994).

Based on these observations, the properties of both natural and synthetic anatases were studied using chemical and thermal analysis, X-ray diffraction, and Mössbauer-, electron spin resonance- and FTIR-spectroscopy to obtain more conclusive evidence regarding Fe-for-Ti-substitution in this mineral.

MATERIALS AND METHODS

Four saprolite samples (II 1; II 2; II 5; IV 6a) formed from basalts in central Nigeria (Zeese *et al* 1994) and one (In15) from a biotite gneiss from south India (Schwertmann 1984) were examined. Pedogenic anatase concentrates were prepared from the kaolinitic-goethitic-hematitic saprolites by first removing the Fe oxides with DCB (Mehra and Jackson 1960). Kaolinite was subsequently dissolved using first hot 5 M NaOH and then cold 0.5 M HCl to remove sodalite and possible Fe oxides formed from kaolinite-Fe during NaOH treatment. For comparison, five euhedral, dipyramidal, non-pedogenic anatase crystals 1–3 mm in length from various museum collections were analyzed without any pretreatment.

A series of synthetic anatases (series 71) was produced by precipitating mixed FeCl$_3$-TiCl$_4$ solutions with NH$_3$ at pH 5.5 (Fitzpatrick *et al* 1978) and then treating the precipitates hydrothermally in a 200-ml teflon vessel with 100 ml of water at 180°C for 40 hours in an attempt to improve crystallinity. After treatment, the samples were washed with water and freeze-dried. The Fe/(Ti+Fe) ratios of the original solutions were 0; 0.025; 0.05; 0.075; 0.10; 0.125 and 0.2 mol/mol, and the samples were designated as 71/0 to 71/20, accordingly. An additional sample for Mössbauer spectroscopy was prepared with isotopically enriched ^{57}Fe and a Fe/(Ti+Fe) of 0.002 mol/mol. This sample was produced to test if trace amounts of Fe in a TiO$_2$ matrix are homogenously distributed or clusters of Fe oxides. To remove any coprecipitated Fe^{III} oxide in the synthetic samples, 400 mg of each sample were treated twice with 20 ml of 6 M HCl on a sand bath at ca. 100°C for 1 hour, washed twice with 50 ml of 6 M HCl and freeze-dried.

Total Fe and Ti were determined after dissolving ca. 30 mg of both natural and synthetic samples with 2.5
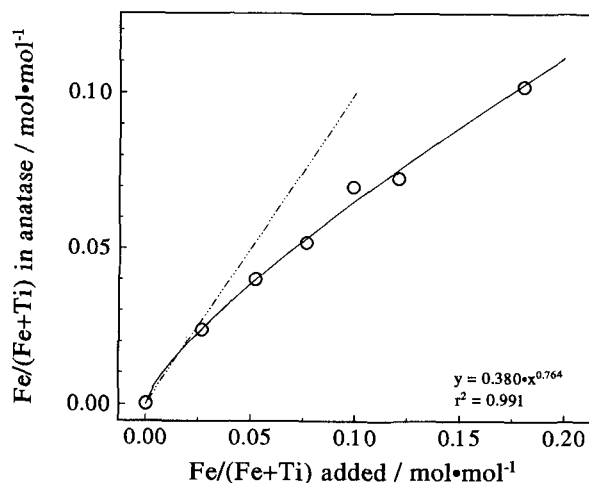
599

Figure 1.   Relationship between the Fe/(Ti+Fe) ratio in synthetic anatases after HCl treatment and the Fe/(Ti+Fe) added.
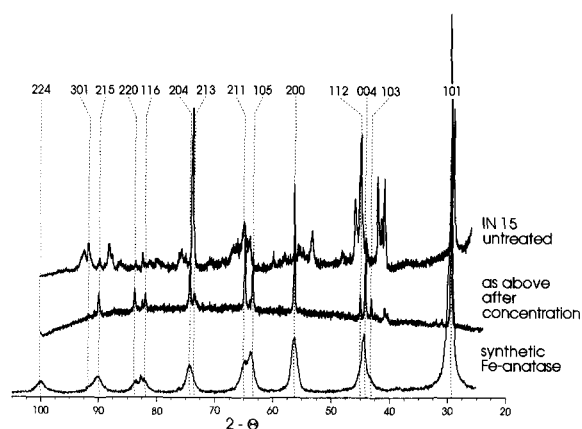

Figure 2.   XRD traces of sample IN15 from a saprolite before and after DCB and NaOH treatment for anatase concentration and of a synthetic anatase 71/12.5. The figures denote the Miller indices of anatase.

ml conc. H_2SO_4 in a 50 ml beaker on a sand bath (requires ca. 1 hour). Ti was determined photometrically with tiron and Fe with o-phenanthroline (Köster 1979). To neutralize excess H_2SO_4, solid Na acetate was added until the red color of the Fe-o-phenanthroline complex developed. The weight loss of the synthetic samples was measured by heating parts of them at 200°C and 850°C for 14 hours. Other parts heated to various temperatures up to 800°C for 19 hours were X-rayed, and Mössbauer spectra were collected on selected specimens.

X-ray diffractograms (XRD) of top fill powder mounts of the synthetic samples were obtained after adding 10% Si as an internal standard by using Co-K_α radiation with a Philips PW 1820 goniometer equipped with a diffracted beam monochromator and a 1° divergence slit. The samples were step-scanned from 25° to 105° 2θ with a step size of 0.05° 2θ and 20 s counting time per increment. Diffractograms of the natural samples were taken using Co-K_α radiation with a Guinier goniometer (Huber, D-83253 Rimsting). These samples were step-scanned from 25° to 100° 2θ with a step size of 0.04° 2θ and 20 s counting time or from 20° to 100° 2θ with a step size of 0.01° 2θ and 10 s counting time. The scans were fitted with the FIT program of Janik and Raupach (1977) as modified by H. Stanjek (this institute, unpubl. data). Unit cell edge lengths, *a* and *c,* of the tetragonal cell were calculated with the program GITTER (W. Hummel, unpubl. data) using the 101, 004, 200, 105, 211, 204, 116 and 220 reflections and a tan θ-weighting. Mean coherence length of crystals perpendicular to a given hkl plane (MCL_{hkl}) was calculated from the corrected integral width b_{corr} at half intensity using the Scherrer formula: $MCL_{hkl} = K\lambda/b_{corr} \cos \theta$ (λ = X-ray wave length, K = constant). Transmission electron micrographs (TEM) were ob-

tained with a Zeiss EM 1OA/B electron microscope, and FTIR spectra were obtained with a Nicolet Magna 550 instrument. Mössbauer spectra were recorded at room temperature and at 4.2 K in transmission geometry with a source consisting of ^{57}Co in a Rh-matrix. The source was vibrated with a sinoidal wave form. For the room temperature spectra, both source and absorber were at 298(4) K. A liquid helium bath cryostat was used to cool both source and absorber to 4.2 K. Electron paramagnetic resonance (EPR) spectroscopy was performed on the untreated sample 71/7.5 and after heating the sample at 500°C for six hours. The EPR spectra were recorded on a Bruker ESP 300 spectrometer equipped with cryogenic system and operating at X-band frequency with 100 kHz magnetic field modulation. The spectrometer settings were 1 or 2 mW microwave power, 0.5 T field modulation amplitude and 9.38 GHz frequency. Spectra were recorded at RT and at 4.7 K. To determine the g-values N,N-diphenylpicrylhydrazyl (DPPH) as reference was used.

RESULTS AND DISCUSSION

Mineralogic and chemical composition

All synthetic samples were monophase anatase after HCl treatment, which removed a reddish stain of hematite (see below). After this treatment, the Fe/(Ti+Fe) ratio ranged between 0.0 and 0.10 mol/mol and the color graded from white into light yellow as the Fe content increased. The proportion of Fe taken into the solid phase increased degressively with increasing Fe/(Ti+Fe) of the original solutions (Figure 1).

As seen from a comparison of XRD traces of the saprolites before and after the concentration procedure (Figure 2), the concentrates consisted essentially of anatase. Where initially present, quartz was the only identifiable impurity left. Only one sample (IV 6a) con-
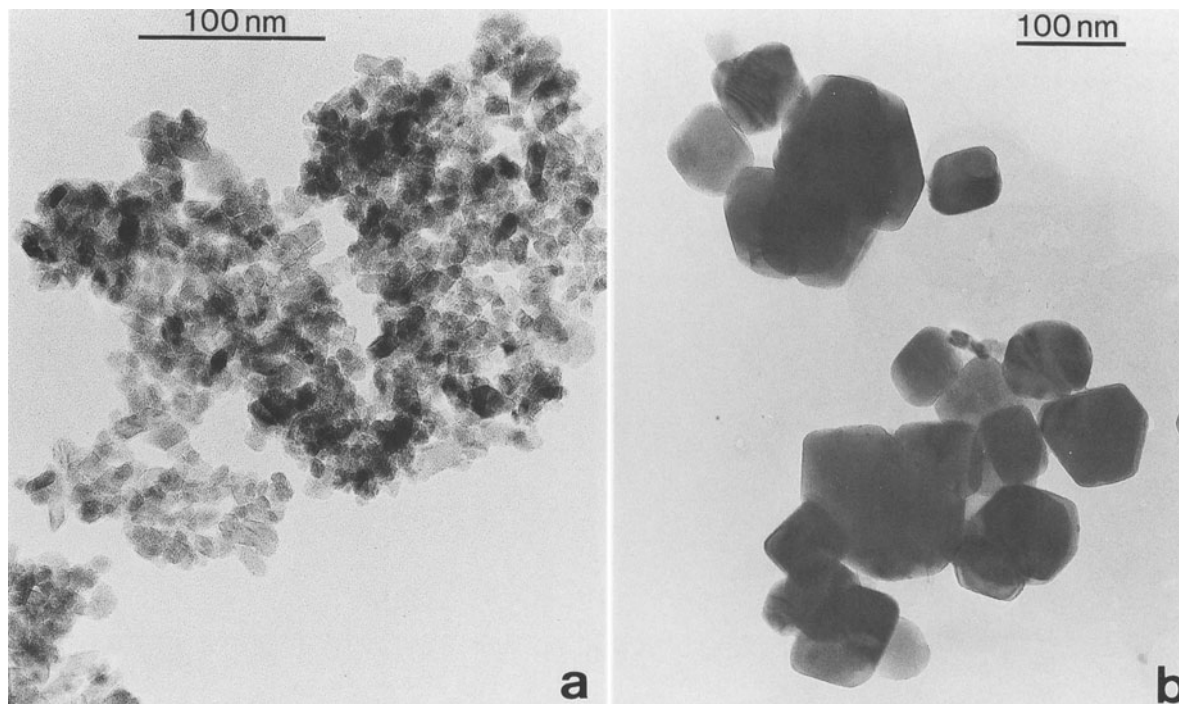
Figure 3. Electron micrographs of a synthetic (71/20, a) and a soil anatase (In15, b).

tained small amounts of pseudorutile, $Fe_2Ti_3O_9$, as indicated by broad XRD lines at 0.25, 0.219 and 0.169 nm and by a Mössbauer spectrum at 4.2 K showing a magnetic hyperfine pattern with a field of 43.9 T too low for any of the Fe oxides. Because this sample contained a second Fe-bearing phase, its Fe content was higher than expected from the unit cell size of its anatase. The sample was, therefore, excluded from further analysis.

Crystal size and unit cell edge length

The crystal size of the synthetic anatases was around 10 nm (Figure 3a). Correspondingly, the X-ray reflections were broadened (ca. 1° 2θ, Figure 2) and the MCL_{101} had an average value of 7.6 ± 1.0 nm. This indicates that XRD line broadening was essentially due to small particle size. In contrast, MCL_{101} of the soil anatases ranged between 87 and 112 nm in agreement with the electron micrograph (Figure 3b).

The edge length c of the tetragonal unit cell of the synthetic anatase showed a regular, statistically significant increase with increasing Fe (Table 1), whereas both the museum and the soil anatases had essentially equal and relatively high c-values and could, therefore, not be included in the regression. A low sensitivity or even an erratic behaviour of c compared to a, i.e., perpendicular to as against within the oxygen sheets, was also observed for Al-substituted hematite (Schwertmann *et al* 1979, Stanjek and Schwertmann 1992).

Such an irregular structural response perpendicular to the oxygen sheets suggests stacking defects that are possibly due to the incorporation of structural OH (see below). Extra OH was also found to be responsible for a similar erratic behaviour of Al goethites (Schwertmann and Carlson 1994).

In contrast to c, the edge length a of the tetragonal unit cell of synthetic anatase (Figure 4a) and the cell volume V (Figure 4b) increased linearly from 0.3785 nm to 0.3810 nm and from 0.1366 to 0.1385 nm^3, respectively, as Fe/(Ti+Fe) increased from 0 to 0.102 mol/mol. The a-values of soil anatases appear to fall on the same correlation line. It may be noticed that the comparison between the synthetic and soil anatases is somewhat hampered by the significant difference in line broadening. Correction for this would be helpful but no correction functions are presently available for the anatase structure.

Table 1. Regression parameters for the correlation between Fe content and unit cell parameters of natural and synthetic anatases.

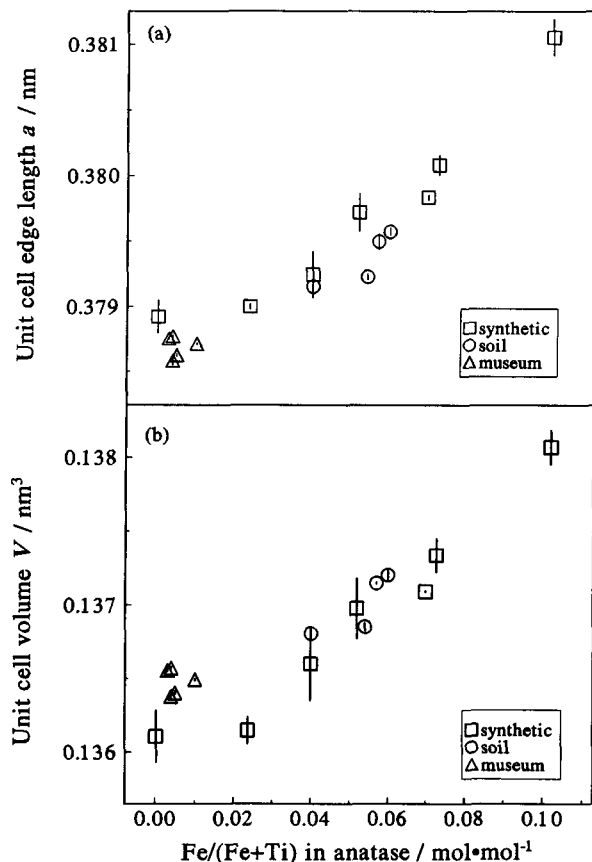| Sample set	Parameter*	n	Intercept	Slope	r^2
All	a	16	0.37856	0.0194	0.858
	V	16	0.13624	0.0143	0.807
Synthetic	a	7	0.37862	0.0210	0.910
	c	7	0.94788	0.0338	0.836
	V	7	0.13588	0.0200	0.944

* a, c in nm; V in nm^3.

Figure 4. Unit cell edge length *a* (a) and cell volume *V* (b) of museum, soil and synthetic anatases as a function of their Fe/(Ti+Fe) ratio. Vertical bars indicate standard deviation.
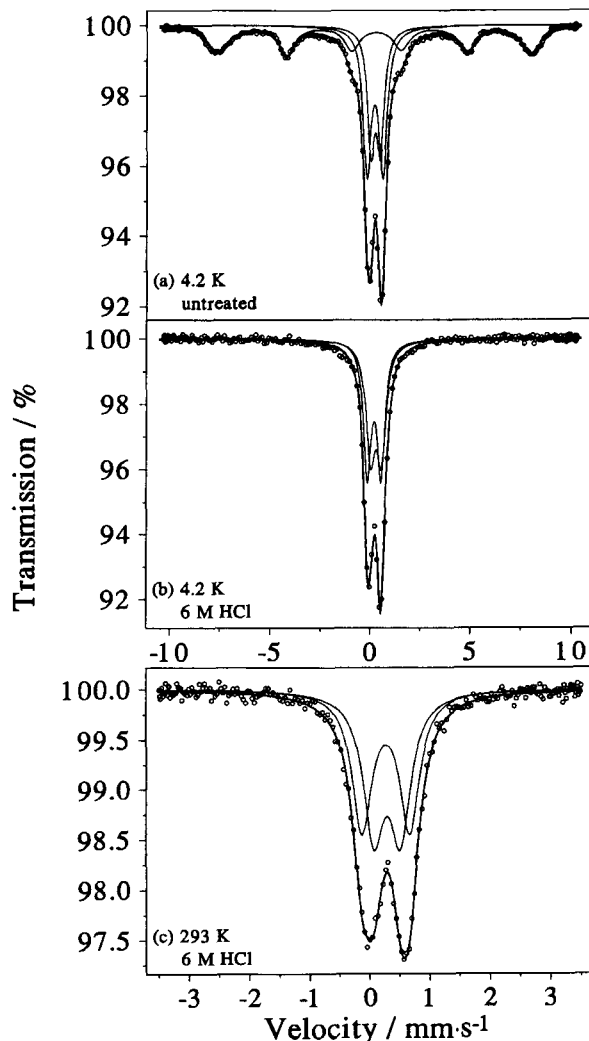

Figure 5. Mössbauer spectra at 4.2 K of sample 71/12.5 before (5 a) and after treatment with 6 M HCl (5 b) to remove hematite. The 293 K spectrum (5 c) shows the doublet at an expanded scale.

We conclude from this that the uptake of Fe has led to a consistent increase in the cell size of anatase (Table 1, Figure 4). The observed increase in the unit cell edge length *a* by 0.7% for Fe/(Ti+Fe) = 0.1 can be predicted from the size of the Fe^{III}-cation in octahedral coordination, which is ca 7% larger than that of octahedral Ti^{IV} (0.0645 vs. 0.06050 nm). In other words, the Vegard rule is approximately followed.

Electronic environment of Fe

All Mössbauer spectra of Fe-containing synthetic anatases at room temperature as well as at 4.2 K showed one asymmetric doublet with isomer shifts typical for Fe^{III}. As an example, Figure 5 shows the spectra at 4.2 K and RT of sample 71/12.5. Without pretreatment the 4.2 K spectrum of 71/12.5 showed a broadened, weak sextet due to hematite (Figure 5a) that was removed by HCl treatment without altering the doublet (Figure 5b). Within statistical uncertainty, both lines of the doublet have identical areas, whereas the line widths are different and substantially broadened (Figure 5c). The observation of one doublet Mössbauer

resonance that is stable with temperature is indicative of Fe^{III} dispersed in the anatase structure. Although the doublet can be described rather satisfactorily by a gaussian distribution of symmetrical doublets of lorentzian lines, a slightly better fit is obtained by superimposing two symmetrical doublets of lorentzian lines with free widths and different isomer shifts and quadrupole splittings. The results of such fits for all anatases are compiled in Table 2.

The asymmetry of the doublet which also existed in the soil anatases can not yet be satisfactorily explained. Among the possible explanations are different environments of Fe^{III} due to incorporation of OH (see below). Further support for the dispersion of Fe^{III} in the anatase structure is derived from the spectra of the sample doped with a trace amount of ^{57}Fe (Fe/(Ti+Fe)

Table 2. Mössbauer parameters at RT of synthetic and soil anatases with different concentrations of structural Fe. Area is the fractional intensity, W the lorentzian line width, QS the electrical quadrupole splitting and IS the isomer shift with respect to a source of ^{57}Co in Rh. For measuring 70/8 BP the sample was diluted with benzophenone $(C_{10}H_{13}O)$ to suppress orientation. The value denoted with (*) was kept constant to obtain a stable fit.

Sample	QS mm·s^{-1}	IS mm·s^{-1}	W mm·s^{-1}	Area %
70/8	0.40(3)	0.29(1)	0.38(3)	37(7)
	0.74(2)	0.27(1)	0.46(8)	63(7)
70/8 BP	0.42(3)	0.29(1)	0.39(3)	45(9)
	0.76(3)	0.27(1)	0.43(2)	55(9)
71/2.5	0.46(1)	0.28(1)	0.45(3)	65(11)
	0.74(11)	0.22(2)	0.82(6)	35(11)
71/7.5	0.50(3)	0.28(1)	0.42(2)	56(8)
	0.85(3)	0.26(1)	0.45(2)	44(8)
71/7.5	0.51(3)	0.29(1)	0.46(3)	73(15)
	0.82(7)	0.25(2)	0.46(5)	27(15)
71/12.5	0.44(3)	0.29(1)	0.42(2)	51(5)
	0.79(2)	0.27(1)	0.40(*)	49(5)
71/20	0.54(2)	0.28(1)	0.42(1)	68(6)
	0.89(2)	0.26(1)	0.39(2)	32(6)
In 15	0.52(3)	0.27(1)	0.34(6)	32(18)
	0.74(6)	0.24(1)	0.55(3)	68(18)

= 0.002, Figure 6). Its 293 K spectrum exhibited a very wide resonance (Figure 6b) without any structure except for two differently broadened peaks at −0.1 and +0.4 mm·s^{-1} (Figure 6a). Such ^{57}Fe-Mössbauer resonance is typical for slow electronic relaxation (Wickman *et al* 1966), which is confirmed by the appearance of hyperfine splitting at 4.2 K demonstrating the effect of temperature on the relaxation time. For ^{57}Fe, relaxation of the electronic spin is usually faster than the lifetime of the excited Mössbauer state (141 ns). In magnetically dilute materials, interactions between the spins may, however, be so weak that the electronic relaxation rate is slowed down to an extent which leads to a magnetic splitting (slow paramagnetic relaxation). At low temperatures this phenomenon can cause hyperfine splittings that often resemble those obtained in magnetic hyperfine fields up to 55 T.

At higher temperatures the relaxation rate increases, but in some cases paramagnetic hyperfine splittings or at least substantial line broadening caused by intermediate relaxation rates persist even at room temperature. When fitted with relaxation lines as given by Wickman *et al* (1966), one set of hyperfine patterns corresponding to high spin Fe^{III} yields good correspondence to the 4.2 K as well as to the RT spectrum (Figure 6a and b), but does not reproduce the doublet structure found in the center (Figure 6a) showing that the model applied cannot describe these relaxation mechanisms in detail. The set of hyperfine parameters of the well resolved sextet of Figure 6c is IS = 0.28(1)
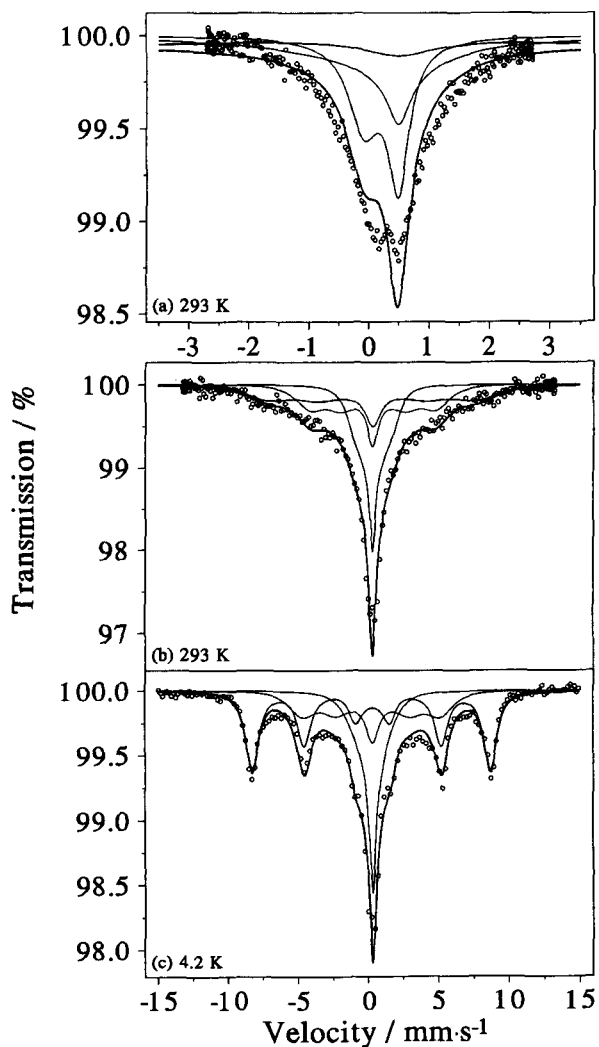

Figure 6. Mössbauer spectra of $Ti_{0.998}{}^{57}Fe_{0.002}O_2$ (a) at 293 K; (b) at 293 K with compressed scale and (c) at 4.2 K.

mm·s^{-1}, EQ = −0.12(1) mm·s^{-1} and a hyperfine splitting equivalent to a magnetic field B = 52.8(1) T. These values differ from those of hematite or any other Fe^{III} oxide, but they are typical for slow relaxation of Fe^{III} diluted in a diamagnetic matrix, viz. TiO_2 here. Thus Fe^{III} structure bound in anatase can be postulated.

The EPR spectrum of sample 71/7.5 at RT showed a weak signal at g = 4.3 and an overlay of a broad and a narrower signal at g = 2 (Figure 7a). Upon cooling to 4.7 K, the latter signal with a line width of 31.5 mT increased in intensity and became sharper. A similiar behaviour with temperature was found for the resonance at g = 4.3. In mineral phases, such EPR signal at low-fields is characteristic for Fe^{III} ions in distorted coordination polyhedra of rhombic symmetry (McBride 1990). Since in anatase TiO_6 octahedra are distorted, the interpretation agrees well with previous
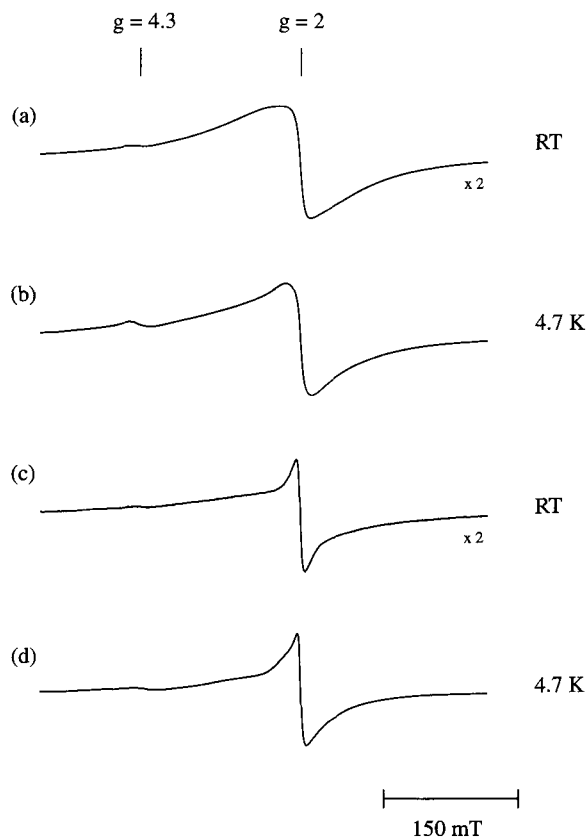
Figure 7.   EPR spectra of the sample 71/7.5 measured at RT (a) and 4.7 K (b); and after heat treatment of the sample at 500°C for 12 h (c, d).

Figure 8.   The effect of heating on the integral width at half height (a) and the unit cell edge length *a* (b).

studies on Fe^{III} doped TiO_2 polymorph rutile, which showed similar lowfield resonance (Thorp 1986).

The assignment of the narrow signal at $g = 2$ is less certain (Figure 7b). Fe^{III} in an undistorted octahedral ligand field can cause resonance at $g = 2$ (Gehring *et al* 1990). Gainon and Lacroix (1962) found such a resonance for structure bound Fe^{III} in a single crystal of a natural anatase. It is, therefore, likely that the narrower signal at $g = 2$ is due to Fe^{III} located in undistorted octahedral sites of anatase. The broad resonance centered near $g = 2$ can be explained by means of an Fe^{III}-rich inclusion in the anatase, since no Fe^{III} oxide in sample 71/5 was found by Mössbauer spectroscopy.

Upon heating the sample to 500°C, the intensities of all signals decreased (Figure 7c and d). The resonance at $g = 4.3$ had almost disappeared. The line width of the signal at $g = 2$ narrowed to a value of 27.5 mT. The narrowing of the line width indicated a weaker dipole-dipole interaction between Fe^{III} cations in the heated sample and can be explained by the release of Fe^{III} from the anatase structure. In agreement with Mössbauer spectroscopy, no Fe^{III} oxides were detected by EPR.
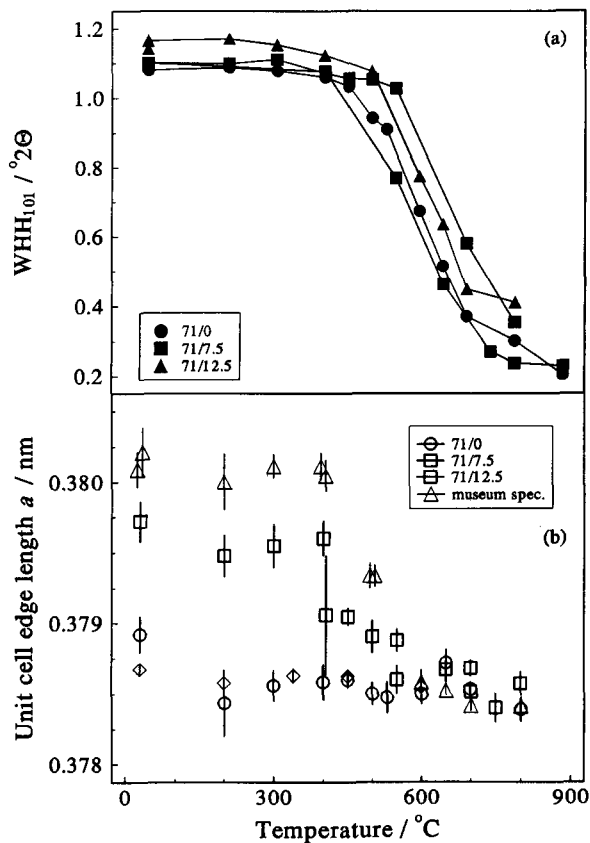
Thermal behavior

Upon heating to between 500°C and 600°C, the X-ray reflections of synthetic anatases sharpened considerably as seen from a drastic decrease in the width at half height (Figure 8a). The MCL_{101} of Fe-substituted anatase increased from 7.6 ± 1.0 to 19.0 ± 3.0 nm, and the unit cell edge lengths *a* were reduced to that of the Fe-free synthetic (71/0) and museum anatase (Figure 8b).

This result suggested that structural Fe had been expelled, but neither X-ray diffractograms nor Mössbauer spectra of the heated samples showed the formation of hematite or any other pure Fe oxide. Instead, all six XRD lines of pseudobrookite, Fe_2TiO_5, with relative intensities $I/I_0 > 10$ appeared, viz. 100, 230, 200, 002, 331, 131, 301 and 232. This agreed with the Mössbauer spectrum at RT of sample 71/12.5 after heating to 800°C, where pseudobrookite was indicated by a less asymmetric doublet with isomer shift IS = 0.27 mm·s^{-1} and quadrupole splitting EQ = 0.73 mm·s^{-1}, which could best be fit with a gaussian distribution of symmetrical, lorentzian doublets (Figure 9a). The 4.2 K spectrum (Figure 9b) showed a dominant (areal
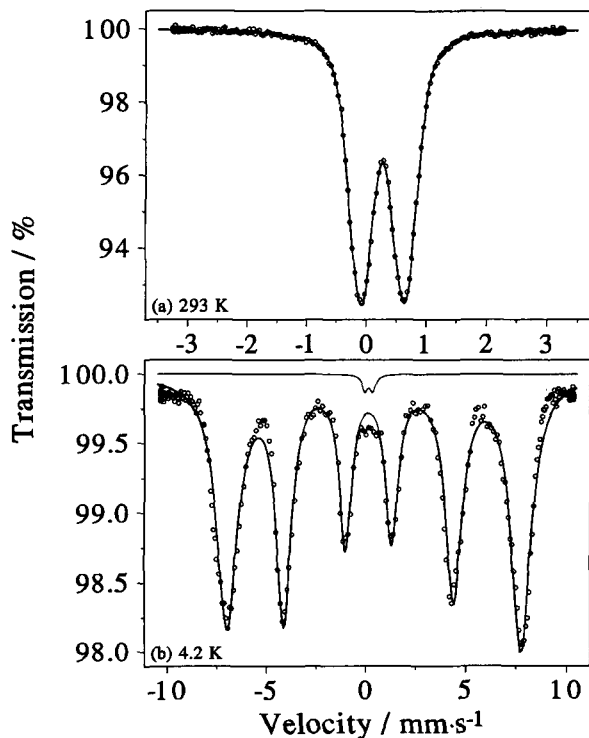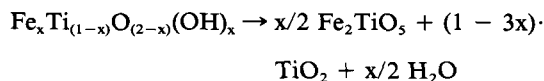
Figure 9. Mössbauer spectra of sample 71/12.5 heated at 800°C for 8 hour (a) 293 K spectrum (b) 4.2 K spectrum.

Figure 10. FTIR spectra of Fe-free (71/0) and Fe-containing anatase before (71/12.5 and 71/20) and after (71/20) heating to 600°C.

intensity 95(1)%), asymmetric, magnetically ordered component with a hyperfine field $B_{HF} = 45.9(1)$ T and very broad non-lorentzian lines when fitted with one sextet of individual line widths. This was assigned to pseudobrookite. The RT-doublet and 4.2 K-sextet of pseudobrookite were also detected, but were less intense (81(1)%) after heating at 600°C for 6 h. From these results we conclude that on heating, structural Fe in anatase segregated according to the following reaction:

$$Fe_xTi_{(1-x)}O_{(2-x)}(OH)_x \rightarrow x/2\ Fe_2TiO_5 + (1-3x)\cdot$$

$$TiO_2 + x/2\ H_2O$$

The pure TiO_2 phase was either anatase or a mixture of anatase and rutile. The proportion of rutile increased with increasing temperature.

Charge balance

In the above equation, it is assumed that the deficit of positive charge in the structure of Fe-anatase is balanced by protons, i.e., structural OH. FTIR spectra of Fe containing anatases showed, beside bands for molecular H_2O at 3400 and 1600 cm^{-1}, weak bands at ca. 3360 and 960 cm^{-1} (Figure 10), which can be assigned to OH stretching and bending, respectively. Both bands were absent in sample 71/0 and disappeared after heating to 600°C in agreement with the ejection of structural Fe.
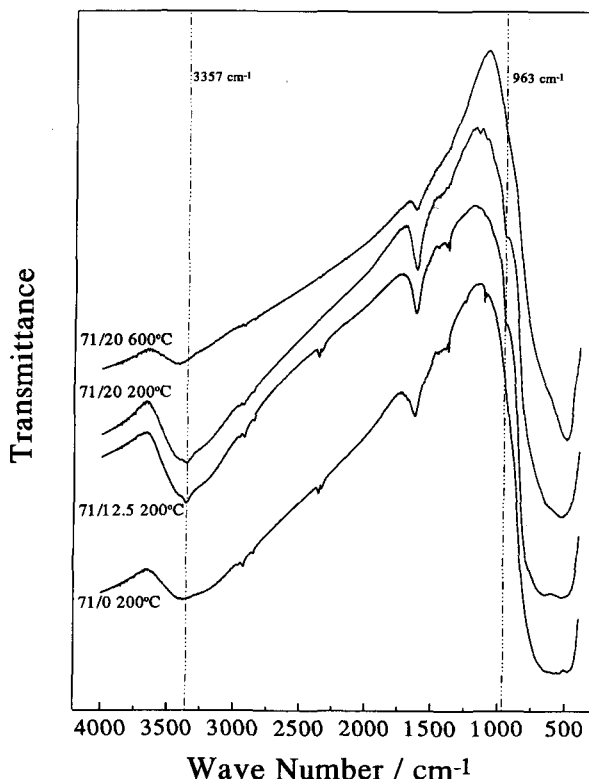
A quantification of OH was attempted by measuring the weight loss between 220°C and 800°C, expressed as mole H_2O/kg and corrected for the weight loss of sample 71/0, which was treated as a blank assuming that all other samples had the same weight loss non-associated with Fe-for-Ti substitution. As Table 3 shows there is a significant positive relation ($r^2 = 0.91$) between the Fe substitution and the extra water content (last column), and the slope is close to 0.5 mole H_2O/

Table 3. Molar ratio (Fe/(Ti + Fe), overall Fe and H_2O content of synthetic anatases 71/0–71/20. The H_2O content was taken equal to the difference by weight between 220°C and 800°C. Due to lack of sample it could not be determined for 71/7.5.

Sample	Fe/(Ti + Fe) mol·mol^{-1}	Fe content 220°C mol·kg^{-1}	H_2O content 220°C–800°C	
			Absolute mol·kg^{-1}	Difference to 71/0 mol·kg^{-1}
71/0	0.0002	0.003	1.70	0.00
71/2.5	0.0237	0.297	1.75	0.05
71/5	0.0400	0.498	1.79	0.09
71/7.5	0.0519	0.654	n.d.	n.d.
71/10	0.0698	0.871	1.97	0.27
71/12.5	0.0726	0.916	2.12	0.42
71/20	0.1019	1.225	2.28	0.58

mole Fe as can be expected from the above reaction. We conclude that this H_2O originated from structural OH-groups incorporated in the anatase structure as a consequence of the substitution of Fe for Ti, thereby compensating for the positive charge deficit. As the Fe is ejected from the anatase structure with heating, so is OH.

CONCLUSIONS

The main question to be answered in this study was whether or not Fe in synthetic and pedogenic anatase could replace structural Ti. Strong support for such an isomorphous replacement was provided by the increase in the unit cell parameters a and V with increasing Fe content, and by the decrease of a and V to the values of pure anatase when the structural iron was ejected to form pseudobrookite, Fe_2TiO_5. The replacement of Ti by Fe in anatase was also supported by Mössbauer and EPR spectra indicating structural Fe^{III} rather than a separate Fe-Ti-O-phase, which was formed when structural Fe was ejected. Replacement of Ti^{IV} by Fe^{III} created a negative charge that was balanced by an $O \rightarrow OH$ transformation, as shown by FTIR and weight loss measurements. Most likely, substitution of some Ti by Fe^{III} is typical for pedogenic anatases as compared to hydrothermal or other lithogenic ones.

ACKNOWLEDGMENTS

REFERENCES

Deer, W. A., R. A. Howie, and J. Zussman. 1962. *Rock-forming minerals. Vol. 1–5.* London: Longmans, Green & Co. Ltd.

Fitzpatrick, R. W., J. Le Roux, and U. Schwertmann. 1978. Amorphous and crystalline titanium and iron-titanium oxides in synthetic preparations, at near ambient conditions, and in soil clays. *Clays & Clay Miner.* **26**: 189–201.

Gainon, D., and R. Lacroix. 1982. Electron paramagnetic resonance of Fe^{3+}-Ion in anatase. *Proc. Phys. Soc.* **79**: 658–659.

Gehring, A. U., R. Kathrein, and A. Reller. 1990. Activated state in the lepidocrocite structure during thermal treatment. *Naturwissenschaften* **77**: 177–179.

Gurewitz, E., and U. Atzmony. 1982. Mössbauer-effect study of Fe_2TiO_5, an anisotropic uniaxial spin-glass. *Phys. Review B, Vol. 26, No.* **11**: 6093–6098.

Janik, L. J., and M. Raupach. 1977. An iterative, least-squares program to separate infrared absorption spectra into their component bands. *CSIRO (Austr.) Div. Soil Tech. Pap.* **35**: 1–37.

Köster, H. M. 1979. *Die chemische Silikatanalyse.* Berlin, Heidelberg, Springer, New York: 196 pp.

McBride, M. 1990. Electron spin resonance spectroscopy. In *Instrumental Surface Analysis of Geological Material.* D. L. Perry, ed. New York: VCH Publisher, 233–281.

Mehra, O. P., and M. L. Jackson. 1960. Iron oxide removal from soils and clays by a dithionite-citrate system buffered with sodium bicarbonate. *Clays & Clay Miner.* **7**: 317–327.

Milnes, A. R., and R. W. Fitzpatrick. 1989. Titanium and zirconium minerals. In *Minerals in Soil Environments,* 2nd ed. J. B. Dixon and S. B. Weed, eds. *Soil Sci. Soc. Am. Book Series No.* **1**: 1131–1205.

Schwertmann, U. 1984. Iron oxides in some ferruginous soils of India. *Clay Res.* **3**: 23–30.

Schwertmann, U., and L. Carlson. 1994. Aluminum influence on iron oxides: XVII. Unit cell parameters and aluminum substitution of natural goethites. *Soil Sci. Soc. Am. J.* **58**: 256–261.

Schwertmann, U., R. M. Fitzpatrick, R. M. Taylor, and D. G. Lewis. 1978. The influence of aluminum on iron oxides. II. Preparation and properties of Al-substituted hematites. *Clays & Clay Miner.* **27**: 105–112.

Stanjek, H., and U. Schwertmann. 1992. The influence of aluminum on iron oxides. Part XVI: Hydroxyl and aluminum substitution in synthetic hematites. *Clays & Clay Miner.* **40**: 347–354.

Teller, R. G., M. R. Antonio, A. E. Grau, M. Gueguin, and E. Kostiner. 1990. Structural analysis of metastable pseudobrookite ferrous titanium oxides with neutron diffraction and Mössbauer spectroscopy. *Solid State Chem.* **88**: 334–350.

Thorp, J. S., H. S., Eggleston, T. A. Egerton, and A. J. Pearman. 1986. The distribution of iron centres in Fe-doped rutile powders. *J. Mater. Sci. Lett.* **5**: 54–56.

Wickman, H. H., M. P. Klein, and D. A. Shirley. 1966. Paramagnetic hyperfine structure and relaxation effects in Mössbauer spectra: ^{57}Fe in ferrichrome A. *Phys. Rev.* **152** No. 1: 345–357.

Zeese, R., U. Schwertmann, G. F. Tietz, and U. Jux. 1994. Mineralogy and stratigraphy of three deep lateritic profiles of the Jos plateau (Central Nigeria). *Catena* **21**: 195–214.